

Soumya K. Srivastava<sup>1</sup>  
 Prashant R. Daggolu<sup>1</sup>  
 Shane C. Burgess<sup>2,3,4,5</sup>  
 Adrienne R. Minerick<sup>1</sup>

<sup>1</sup>Dave C. Swalm School of  
 Chemical Engineering,  
 Mississippi State University,  
 MS, USA

<sup>2</sup>College of Veterinary Medicine,  
 Mississippi State University,  
 MS, USA

<sup>3</sup>Institute for Digital Biology,  
 Mississippi State University,  
 MS, USA

<sup>4</sup>Life Sciences Biotechnology  
 Institute, Mississippi State  
 University, MS, USA

<sup>5</sup>Mississippi Agriculture and  
 Forestry Experiment Station,  
 Mississippi State University,  
 MS, USA

Received March 12, 2008

Revised June 19, 2008

Accepted June 23, 2008

## Research Article

# Dielectrophoretic characterization of erythrocytes: Positive ABO blood types

Dielectrophoretic manipulation of erythrocytes/red blood cells is investigated as a tool to identify blood type for medical diagnostic applications. Positive blood types of the ABO typing system (A+, B+, AB+ and O+) were tested and cell responses quantified. The dielectrophoretic response of each blood type was observed in a platinum electrode microdevice, delivering a field of  $0.025 V_{pp}/\mu\text{m}$  at 1 MHz. Responses were recorded *via* video microscopy for 120 s and erythrocyte positions were tabulated at 20–30 s intervals. Both vertical and horizontal motions of erythrocytes were quantified *via* image object recognition, object tracking in MATLAB, binning into appropriate electric field contoured regions (wedges) and statistical analysis. Cells of O+ type showed relatively attenuated response to the dielectrophoretic field and were distinguished with greater than 95% confidence from all the other three blood types. AB+ cell responses differed from A+ and B+ blood types likely because AB+ erythrocytes express both the A and B glycoforms on their membrane. This research suggests that dielectrophoresis of untreated erythrocytes beyond simple dilution depends on blood type and could be used in portable blood typing devices.

### Keywords:

ABO blood type / Dielectrophoresis / Erythrocytes / Medical diagnostics /  
 Microdevice  
 DOI 10.1002/elps.200800166

## 1 Introduction

The rise of electrokinetics as a separation technique during the past decade has crafted new methods of analysis in medical applications. Dielectrophoresis (DEP), a subclass of electrokinetics, shows potential as a useful tool in developing inexpensive, easy-to-use medical microdevices capable of streamlining emergency medical diagnosis. Blood typing is a simple, yet life-essential diagnostic step preceding blood transfusion in major emergency medical situations. The antigens on the surface of donor blood must match the receiver's blood type or adverse immune responses can cause death in the recipient. The conventional serological methods for blood grouping used are the direct hemagglutination, antigen–antibody combined methods consisting of absorption, absorption elution, absorption inhibition and some other modified method along with histochemical methods [1]. Some methods available include using spectrophotometry to sort blood types, which utilizes antibody-

induced changes in the UV–visible spectra of blood [2]. Advantages of using spectrophotometric method are: blood samples having abnormal spectra can be flagged and targeted for further analysis with no centrifugation required [2]. Magnetophoresis can also be a possibility for separating cells such as infected malarial from healthy erythrocytes. One of the advantages of using this technique is that it allows following mobility of hundreds of single cells in a relatively short period of time [3]. Portability of the power source and cell mobility can be less ideal than for a dielectrophoretic system. However, many blood typing technologies require time, a clinical environment, antibody assays for each blood type; such medical technological methodologies require skilled medical technicians and are not readily portable to emergency sites, which make the whole testing method more expensive and prone to false positives and negatives [1–3]. This paper analyzes a novel technique of using DEP as a tool for distinguishing the positive blood types of the ABO system (A+, B+, AB+, O+). Dielectrophoretic characterizations in lab-on-a-chip devices are far more portable than current techniques.

Microdevices have components on micrometer scales and are custom-made based on their specific application, ranging from microelectromechanical systems to DNA analysis and cellular testing [4]. The dielectrophoretic microdevice design used here was based on the prior microdevices fabricated for studying erythrocyte pearl chain formations with perpendicular platinum electrodes [5].

**Correspondence:** Professor Adrienne R. Minerick, Dave C. Swalm School of Chemical Engineering, 323 President's Circle, P.O. Box 9595, Mississippi State, MS 39762, USA

**E-mail:** minerick@che.msstate.edu

**Fax:** +1-662-325-2482

**Abbreviations:** AC, alternating current; DEP, dielectrophoresis; RBC, red blood cell

Several other designs have been studied for other applications including spiral arrangement of electrodes for cell separations [6], interdigitated microarrays [7] and checkerboard arrangements of electrodes [8]. Analytical micro-devices in various forms are being developed to make complicated multi-step biological analysis simpler [9].

Microdevices have the potential for sample analysis cost reduction and versatility in use [10]. Equipment used to perform medical tests, like a standard hematology panel of hematocrits (erythrocytes, platelet and white blood cell counts), electrolyte balance, hemoglobin, *etc.*, are expensive and range from \$55 to \$95 [11]. Other tests like CD4, which test for HIV, rely on flow cytometers that can cost \$65 000 [12]. The fee for such blood tests outsourced to medical laboratories is about \$40 with medical costs rising annually [12]. In contrast, the cost of microdevices is minimal. As manufacturing of microdevices are scaled up, the price *per* device drops and is expected to cost less than \$3 each [12]. Once optimized, the reliability of data from microdevices is expected to exceed that of current medical laboratories.

The use of the microdevices can be extended to diagnose chronic diseases like sickle cell anemia, which affects 1 in 500 African Americans (1 in 12 carry the sickle cell trait) [13]. Diagnosis of sickle cell anemia requires expensive medical kits ranging from \$69 to \$175 each along with the help of skilled medical technicians [14]. Medical micro-devices have the potential to improve upon this by enabling point of care testing in less than 5 min, with only 1–3 drops of blood (~62  $\mu$ L) while simultaneously eliminating human error. DEP is expected to play a major role in development of medical microdevices due to operational simplicity, lack of need for skilled medical technicians, small sample volumes and low voltage signals, all of which enable device portability.

## 1.1 Theory

DEP is a phenomenon, which results in movement of polarizable particles in non-uniform alternating current (AC) electric fields. The movement is due to a net force,  $\vec{F}_{\text{DEP}}$  resulting from transient polarization of particles [15] and the electric field [16]:

$$\vec{F}_{\text{DEP}} = 2\pi r^3 \epsilon_m \alpha \nabla \vec{E}^2 \quad (1)$$

The particle radius is  $r$ ,  $\epsilon_m$  is the medium permittivity,  $\vec{E}$  is the electric field strength and  $\alpha$  is the real part of the Claussius–Mossotti factor, which is the effective polarizability of the particle relative to the suspending medium and is frequency dependent.

$$\alpha = \text{Re}[K(\omega)], \quad K(\omega) = \frac{\tilde{\epsilon}_p - \tilde{\epsilon}_m}{\tilde{\epsilon}_p + 2\tilde{\epsilon}_m} \quad (2)$$

where  $\tilde{\epsilon}$  denotes complex permittivity and the subscript  $p$  refers to a lossless dielectric sphere particle suspended in a medium  $m$ . The complex permittivity  $\tilde{\epsilon}$  is given by  $\tilde{\epsilon} = \epsilon - (i\sigma/\omega)$ , which is a function of permittivity,  $\epsilon$ ,

medium electrical conductivity,  $\sigma$ , and the angular frequency,  $\omega$  [15, 16].

Equation (1) is a generalized equation for spherical, homogenous particles, but is not a precise relation of the dielectrophoretic force on erythrocytes because cells are non-homogenous complex biochemical entities with non-uniform distribution of insulating and conducting components. Analytical dielectric modeling has been done to interpret the movement of biological cells in electric fields using either spheres or ellipsoids as an approximation for their shapes, but remain approximations [17]. Further, it was shown that correct cell geometrical parameters are critical for understanding permittivity of cell suspensions [18–20].

The transient polarization of particles results in their movement in the electric field that scales between two extremes depending on the exciting AC frequency. Pohl, in his seminal text “*Dielectrophoresis: The behavior of neutral matter in nonuniform electric fields*” defined these two phenomenological extremes as positive DEP and negative DEP [15]. These two cases arise as a consequence of the polarizability of a uniform composition particle being greater or lesser than the polarizability of the medium in which it is suspended. If the real part of the effective polarizability,  $\text{Re}[\alpha]$  of the particle is greater than that of the medium, then the electric field lines pass through the particle causing a polarization that is slightly skewed due to the spatially varying electric field lines. A resultant force directs the particle to high field density regions and this observed movement is known as positive DEP. If the effective polarizability,  $\text{Re}[\alpha]$  of the particle is less than that of the medium in which it is suspended, spatially non-uniform electric field lines divert around the outside of the particle causing ion depletion at the particle poles and subsequent polarization. The resulting force directs the particle to the low field density regions and this is termed negative DEP [15, 21]. This work examines these more complicated responses with a medically relevant system: erythrocytes expressing membrane antigens based on their blood type. These factors have been shown to influence the motion of the particles in a dielectrophoretic field.

DEP has been studied in detail by researchers over the past few years. In particular, the phenomenon was studied with regards to erythrocytes [5]; it was observed that A+ erythrocytes form pearl chains in a dielectrophoretic field. DEP is also studied to differentiate normal cells from leukemic cells [20], metastatic breast cancer cells [22] and malarial cells [23]. Using a spiral electrode configuration, the dielectrophoretic movement of cells based on health was studied and malarial cells were separated from healthy cells [6]. DEP has also been used to separate white blood cells from erythrocytes [24] and sample preparation for chip-based hybridization assays in an integrated DNA or RNA system [7]. Furthermore, dielectrophoretic field flow fractionation was used to study differential analysis of human leukocytes [25]. However, systematic qualification as a function of blood type has not previously been performed.

## 1.2 RBCs/erythrocytes

Red blood cells (RBCs) or erythrocytes are the most abundant cells found in whole blood and, in a healthy adult male, 42–54% of the blood volume constitutes of erythrocytes. Erythrocytes are biconcave in shape to maximize surface area for gas ( $O_2$  and  $CO_2$ ) transport across their membrane to the interior hemoglobin protein that transiently binds the gases. The diameter of a typical human erythrocyte disk is 6–8  $\mu\text{m}$ , much larger than most other human cells. Their main function is to bind and carry oxygen from the lungs to the tissues in the body and remove  $CO_2$  from the tissues for release in the lungs. The membrane of erythrocytes is composed mainly of proteins, lipids and polysaccharides. Erythrocytes are manufactured in the red bone marrow of large bones, and lack a cell nucleus and have a life span of approximately 120 days in the human body [26].

The antigens responsible for the A, B and O blood types are one of many polysaccharides expressed on erythrocyte surfaces and are important for donor/recipient blood type compatibility [26]. The A and B antigen differ by the type of modification made to an acceptor glycoconjugate. The A antigen terminates in an  $\alpha$  1,3-linked *N*-acetylgalactosamine while B terminates in an  $\alpha$  1,3-linked terminal galactose [27, 28]. O blood type cells have neither modification. According to the ABO blood typing system, there are four base blood types, A, B, AB and O. The presence or absence of a third antigen, termed the Rhesus (Rh) factor determines the positive and negative blood types [29]. The blood type is assigned a “+” or a “–” sign based on Rh presence or absence, respectively. Also, there are complimentary antibodies in the blood plasma (A and B antibodies), which are the recognition helpers of the immune system. The antibody A is present in B blood type plasma (both + and –) and antibody B is present in A blood type plasma (both + and –). O type plasma has both antibodies and AB has neither. Since antibodies are free in the surrounding blood plasma and not bound to the cell surface, they are assumed to not affect dielectrophoretic erythrocyte response.

Erythrocytes have a net negative charge based on their conventional linear electrophoretic behavior [27]. However, the surface charges of erythrocytes rapidly decrease if the blood is stored for more than 6 days. Cell rigidity also increases if stored for more than 6 days, which could be related to the surface charge phenomena [27]. Blood age as well as the storage container can also influence its properties. Hemolysis is less in cells stored in di-2-ethyl hexylphthalate plasticized bags than in butyryl-*n*-triethylcitrate plasticized bags [30].

In this study of work, we show qualitative and quantitative dielectrophoretic responses of erythrocytes based on positive blood types. Erythrocytes were subjected to dielectrophoretic fields of  $0.025 V_{pp}/\mu\text{m}$  at a frequency of 1 MHz [5] for 120 s and cell movements were observed using video microscopy. Quantification of cell movement with time included both the horizontal and vertical movements of

RBCs in a constant dielectrophoretic field. The results have shown dependency on the blood type for dielectrophoretic movement of RBCs for positive blood types. Specific trends for each blood type with time in both horizontal and vertical directions were tabulated.

## 2 Materials and methods

The parameters fixed in this research were frequency of the AC field and field strength. The parameters changed were time in the electric field and time of blood storage. From previous studies, the frequency was maintained at 1 MHz and the electric field strength was maintained at  $0.025 V_{pp}/\mu\text{m}$  [5]. Blood samples were analyzed in the dielectrophoretic field for 3 min on days 0 to 6 in storage. The important steps in the process were microdevice fabrication, experimentation (including microsample preparation), image analysis, quantification and statistical correlation. Each of these steps is discussed in Sections 2.1 through 2.6.

### 2.1 Microdevice fabrication

The dielectrophoretic field was generated within a microdevice using 100  $\mu\text{m}$  platinum electrode wires positioned  $\sim 200 \mu\text{m}$  apart in a perpendicular configuration. This created a spatially non-uniform AC field. The microdevice was constructed by attaching a Hybriwell chamber (HBW 75 and item # 10484908) to a glass microscopic slide thus creating a thin chamber (40 mm  $\times$  21 mm  $\times$  0.15 mm). Platinum wires for electrodes (100  $\mu\text{m}$  od, 99% pure, Goodfellow, PT005127/128) were placed perpendicular to each other (Fig. 1) and the whole chamber was sealed by pressing the adhesive edges of the Hybriwell chamber onto the microscopic slide. The microdevice then had two sample ports that enabled fluid to be introduced and removed. The outer ends of the electrodes were wrapped in conductive foil so that alligator clips from a 33250A Agilent Waveform Generator could be attached. Programming of the generator resulted in a sinusoidal 1 MHz AC electric field in the chamber.

### 2.2 Microsample preparation

Whole blood was drawn from voluntary donors *via* venipuncture by a certified phlebotomist into Becton and Dickinson, 4 mL vacutainers. The donors were randomly selected, but varied in gender, age and ethnicity. The fresh human blood samples were stored in 1.8 mg  $K_2$  EDTA anticoagulant *per* mL of blood in a refrigerator at 5°C. Prior to conducting experiments, well-mixed whole blood was diluted (1:60) using PBS (0.14 M NaCl, 0.02498 M  $KH_2PO_4$ , 0.00907 M  $K_2HPO_4$ ). A 5000  $\mu\text{L}$  stock solution of blood suspension was prepared by mixing 4918  $\mu\text{L}$  of PBS solution

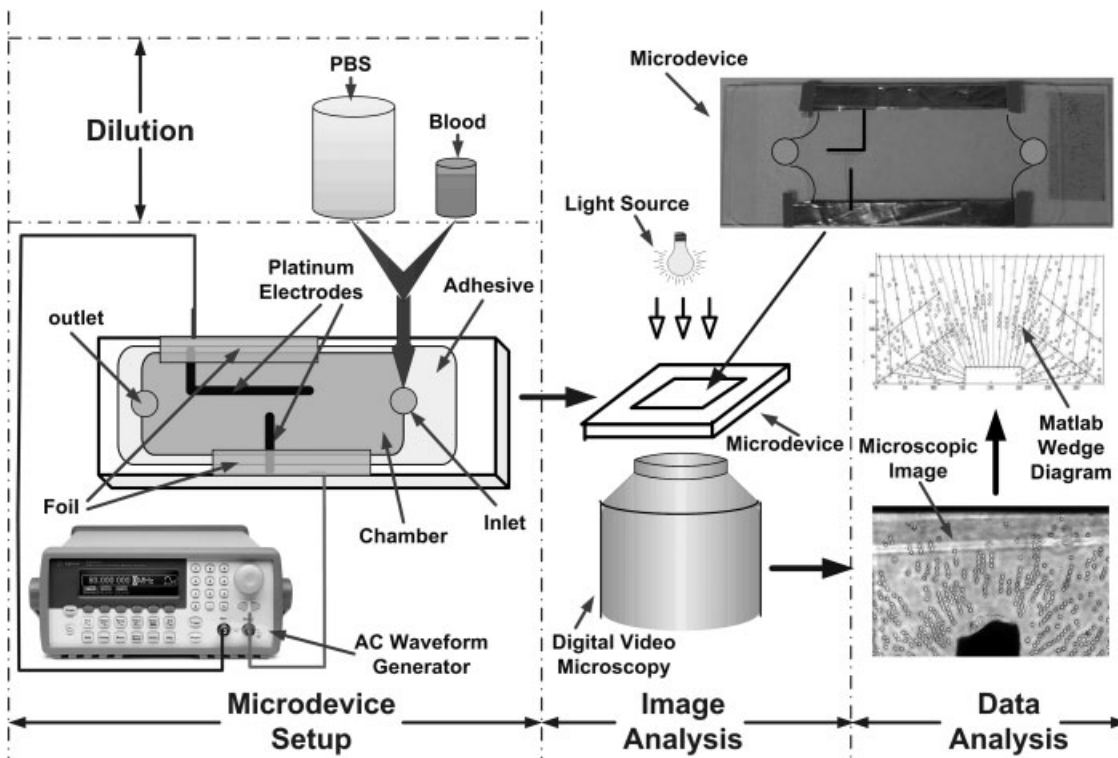


**Figure 1.** Experimental setup illustrating the custom microdevice mounted on an inverted microscope. Microdevice electrodes are connected directly to an AC waveform generator. Sample inlet port is used to introduce dilute blood suspensions. Erythrocyte responses in the dielectrophoretic field are recorded digitally with a high-resolution CCD camera and stored for subsequent image analysis.

and 82  $\mu\text{L}$  of whole blood. The solution was well mixed by gently swirling the mixing vial prior to sample loading into a clean microdevice. The day of the venipuncture was labeled as day 0 and subsequent days were 1, 2, 3, *etc.* For consistency, experiments were performed for three different days and two runs were conducted each day, resulting in six data sets for each condition set and were repeated for the same blood samples at the same conditions.

### 2.3 Experimental procedure

The microdevice was cleaned with e-pure water (Millipore Simplicity Purification System, resistance: 18  $\Omega$ ), inspected under the microscope for any debris, and was rinsed five times with PBS. Diluted blood (about 15  $\mu\text{L}$ ) was micro-pipetted into the microdevice *via* sample ports labeled in Fig. 1. The blood suspension was drawn across the Hybriwell chamber using Kim Wipes, which create a suction from the opposite sample port. This process was repeated five times to ensure that all PBS was displaced with a uniform spatial concentration of the blood suspension throughout the Hybriwell chamber. The sample-filled microdevice was then positioned on the microscope stage and alligator clips were used to connect the foiled platinum electrodes to the waveform generator. A sinusoidal AC frequency of 1 MHz was maintained with electric field

strength of  $0.025 V_{pp}/\mu\text{m}$ , which resulted from an applied voltage of  $5 V_{pp}$  over an electrode gap of 200  $\mu\text{m}$ . Since the distance between electrodes varied between 150 and 200  $\mu\text{m}$ , the applied voltage was adjusted using the following relation to obtain a constant electric field:

$$E = V/d = 0.025 V_{pp}/\mu\text{m} \quad (3)$$

where  $V$  is the voltage of the field in peak-to-peak volts and  $d$  is the distance in micrometers between the electrodes.

The blood suspension in the microdevice was allowed to settle for 10 min while the microscope was focused and video capture settings adjusted. The output from the waveform generator was turned on and after 5 s the video microscopy recording was started. The movement of the erythrocytes was recorded *via* video microscopy at 10 s intervals for 4 min (Fig. 2). These images were compiled and subsequently analyzed to quantify cell motion.

As evident in the electrode profiles in the images in Fig. 2, electrode shape and spacing differed slightly from microdevice to microdevice. Simulations of the electric field were performed in COMSOL Multiphysics [31] and are shown in Fig. 3. Two cases are contrasted. Comparison of Figs. 3A and B demonstrates the significant change in field gradient when the electrode spacing is changed from 200  $\mu\text{m}$  ( $E = 0.03 V_{pp}/\mu\text{m}$ ) to 100  $\mu\text{m}$  ( $E = 0.06 V_{pp}/\mu\text{m}$ ). Darker areas represent high field density regions while lighter areas represent low field density regions.

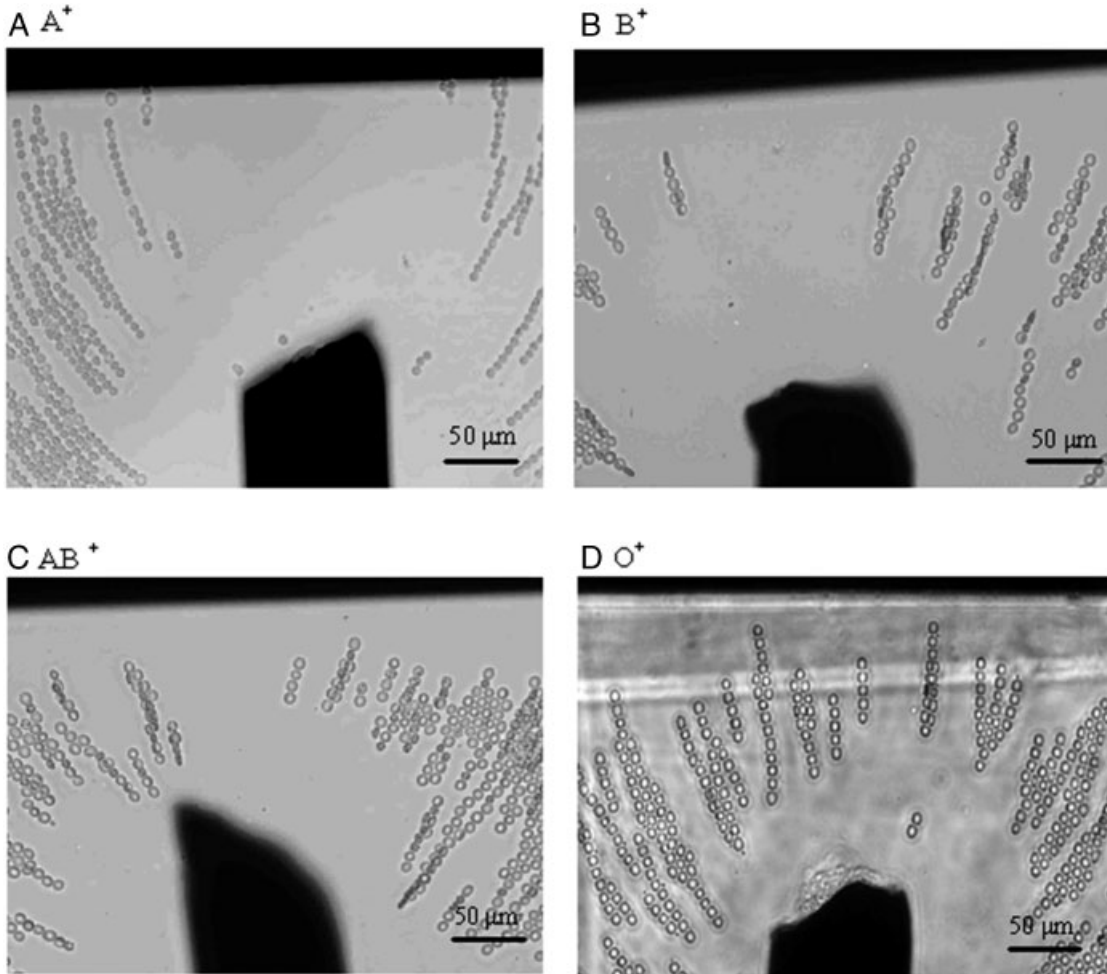


**Figure 2.** Untouched images of erythrocyte distributions in a dielectrophoretic field after 120 s of field application at 1 MHz for (A) A+ blood type, (B) B+ blood type, (C) AB+ blood type and (D) O+ blood type cells. The tip protruding into the bottom of the images is the electrode where field density is the highest and the horizontal dark region at the top of each image is the electrode where density is lowest. RBCs are aligned along field lines between the electrodes. The figure illustrates the difference in orientation of each of the positive ABO blood types studied after 120 s in a 1 MHz,  $0.025 V_{pp}/\mu\text{m}$  AC electric field.

A comparison of Figs. 3C and D illustrate that while symmetry of the field changes slightly with electrode shape, the gradient (the key component in Eq. 1), is not significantly altered. It was concluded that electrode shape is a minor contributor to the field whereas the distance between the electrodes plays a major role in the dielectrophoretic response of erythrocytes. For this reason, considerable effort was dedicated to controlling the electrode spacing in the custom microdevices, but the wire available determined electrode shape.

#### 2.4 Safety considerations

All work was conducted in a certified Biosafety Level II Laboratory with Institutional Biosafety Committee and Institute Review Board approval for human subjects.

#### 2.5 Image analysis

The images were processed with image recognition software (Zeiss Axiovision 4.5) to get X/Y position, cell radius, cell area, bound width and bound height of the cells. Based on the difference in optical intensity of the cells and the image background, this edge recognition software selected cells or cell conglomerates. The software was then programmed to disregard objects that were not cells (either too big or too small). Manual selection of any missed cells occurred with a circle selection tool. For every selected object, the software recorded the following properties: X/Y position, radius, bound height and width in a spreadsheet. The cell count on each time-stamped image for every 10 s was also recorded. The images were analyzed for characteristic differences in their movement every 20–30 s up to 120 s into the experiment.

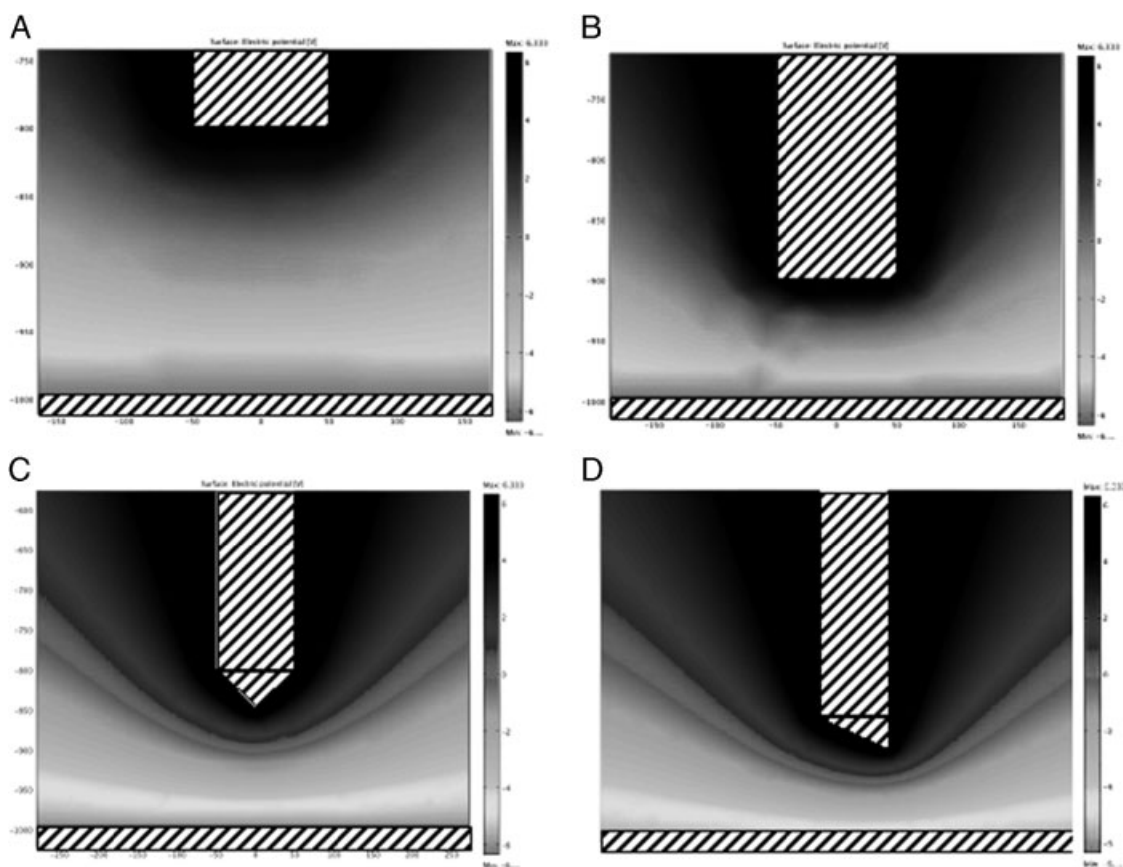


**Figure 3.** Simulations of the electric field in the microdevice were performed in COMSOL Multiphysics. The geometry of the electrode does not affect the separation of erythrocytes (compare Figs. 3A and B) whereas the distance between the high field density region and low field density region electrodes plays a vital role (compare Figs. 3C and D) in determining optimal separation of cells. Dark represents high field density regions while light represents low field density regions.

## 2.6 Data analysis

The *X/Y* data obtained was analyzed for variations with respect to blood type. The first analysis done was a sextant analysis where images were divided into six equal sextants using MATLAB. The sextants were created by dividing the image vertically into two and then horizontally into three. Cell counts were analyzed in each region. However, the sextant approach proved not to be sensitive enough to quantify observed qualitative differences in motion; the regions were too large to show spatial differences in the dielectrophoretic movement of each blood type.

The next binning approach used was a Wedge Analysis where the image was divided into  $\sim 20$  equally sized wedges in a manner such that they approximated electric field lines. In MATLAB, wedge lines from the high field density regions (bottom electrode) to the low field density regions (top electrode) were calculated from a geometry information file containing the dimensions of the high field density electrode, the distance between the electrodes, position of the low field density electrode and resolution of the image. Wedge size was determined by spacing the wedge lines

20  $\mu\text{m}$  apart at the low field density electrode (top region in Fig. 4). Average movement of cells in the vertical and horizontal directions was tabulated for 0, 20, 30, 50, 60, 90 and 120 s for each sample. Data were compiled into a spreadsheet so that averages and standard errors were calculated over days 0, 3 and 5 for each blood sample. Data were further consolidated over independent blood samples for each type. This was done because cell properties do not change appreciably until after 6 days under the storage conditions at 5°C and 1.8 mg  $\text{K}_2$  EDTA [27]. Lastly, a composite parameter that captured the distance that the cells moved in the electric field combined the vertical and horizontal positions *via* the distance formula.

The last approach taken for assessing the significance of the vertical and horizontal movements of RBCs was statistical analysis *via* SAS (Statistical Analysis Software version 9.1) [32]. Analysis of variance and least significance difference with multiple comparisons were performed on both vertical and horizontal movements' data. Analysis of variance was used to assess the primary effects (DAY, TIME and BLOOD TYPE) and the interaction effects of DAY with TIME, DAY with BLOOD TYPE and TIME with BLOOD TYPE. However, it should be noted that in the current study,

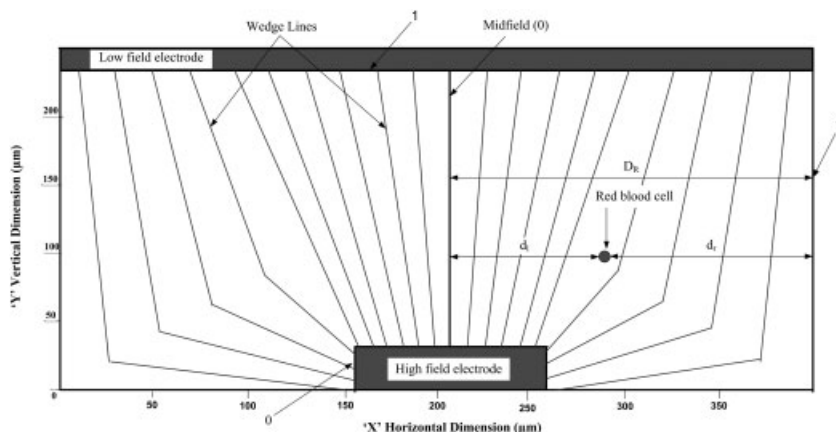


**Figure 4.** Wedge region construct for (X, Y) position tracking in MATLAB. The space between high field density and low field density electrodes was broken into regions approximating the shape of the electric field. These wedge lines are calculated *via* an algorithm and cell movement is then tracked up or down each wedge region (vertical movement) as well as across wedge regions (horizontal movement).

it is not possible to distinguish relative contributions of donor from device variabilities, so repetition dependence was not included in the statistical analysis. The model used for performing the analysis with interaction of the three variables is as follows:

$$Y = (\text{DAY TIME BLOOD TYPE}) \\ (\text{DAY TIME}) (\text{DAY BLOOD TYPE}) \\ (\text{TIME BLOOD TYPE}) \quad (4)$$

Variance was analyzed separately for vertical and horizontal movements. DAY had three parameters 0, 2 and 5; BLOOD TYPE had four parameters A, B, AB and O; TIME had seven parameters 0, 20, 30, 50, 60, 90 and 120. Since the vertical movements of the cells up or down the wedges was tracked separate from the horizontal movement of the cells across wedge lines, the statistical analysis was also conducted on the vertical and horizontal parameters separately.

An analysis of variance and least significant difference was also conducted with multiple comparisons at 60 and 90 s for vertical and horizontal movements respectively, as these were the times where the best spatial separation of blood types were achieved. Hence the model in Eq. (4) was modified by neglecting the interaction effects as shown in the following equation:

$$Y = (\text{DAY TIME BLOOD TYPE}) \quad (5)$$

SAS output was utilized alongside movement data to ascertain whether blood types were distinguishable in a dielectrophoretic field. It aided in calculating the confidence level for distinguishing blood types for different movements depending on the DAY, TIME and BLOOD TYPE.

### 3 Results and discussions

The quantitative and qualitative responses for all four blood types (A+, B+, AB+ and O+) in a  $0.025 V_{pp}/\mu\text{m}$

electric field are presented in this work. The movements are discussed in the context of the traditional Claussius–Mossotti factor prediction of dielectrophoretic motion (Eq. 3) and are found not to be entirely consistent. A set of images for all four positive blood types (A+, B+, AB+, O+) were taken after 120 s of field application and the dielectrophoretic movement was found to be two-dimensional. Figure 2 illustrates the difference in spatial distribution of each of the positive ABO blood types studied, at 120 s after the AC electric field (1 MHz,  $0.025 V_{pp}/\mu\text{m}$ ) was applied. A+ had long chains of cells, which migrated away from the midfield region and were closer to the low field density electrode than the high field density electrode. B+ blood type cells demonstrated shorter chains with significant cell overlap and were positioned away from midfield, as well as the high field density and low field density electrode. AB+ erythrocytes had shorter chains that were agglomerated with some cell overlap. Significant repulsion from the high and low field density electrodes are observed with overall position much closer to the midfield than A+ and B+ blood types. O+ blood group cells had longer chains without overlap and conglomerations.

In order to quantify these different spatial distributions, the time sequence dielectrophoretic erythrocyte responses and mapping in MATLAB for O+ blood type is illustrated in Fig. 5 for 5, 60 and 120 s, respectively. Figures 5A, C and E show the time sequences of untouched images of dielectrophoretic responses. As time progressed, prominent pearl chains and some conglomeration of cells were observed. The cells are closer to the central high field region at 5 s but moved away by 120 s. Similarly, cells at 5 s were closer to midfield whereas at 120 s fewer erythrocytes were closer to the midfield region. Cell position tracking was achieved *via* image analysis object recognition that entailed recording X/Y coordinates of cell position and subsequently exported to MATLAB for binning analysis in wedges (Figs. 4 and 5B, D and F). Comparison between the untouched image and the X/Y position representation *via* MATLAB shows excellent agreement and reinforces that image analysis was reli-

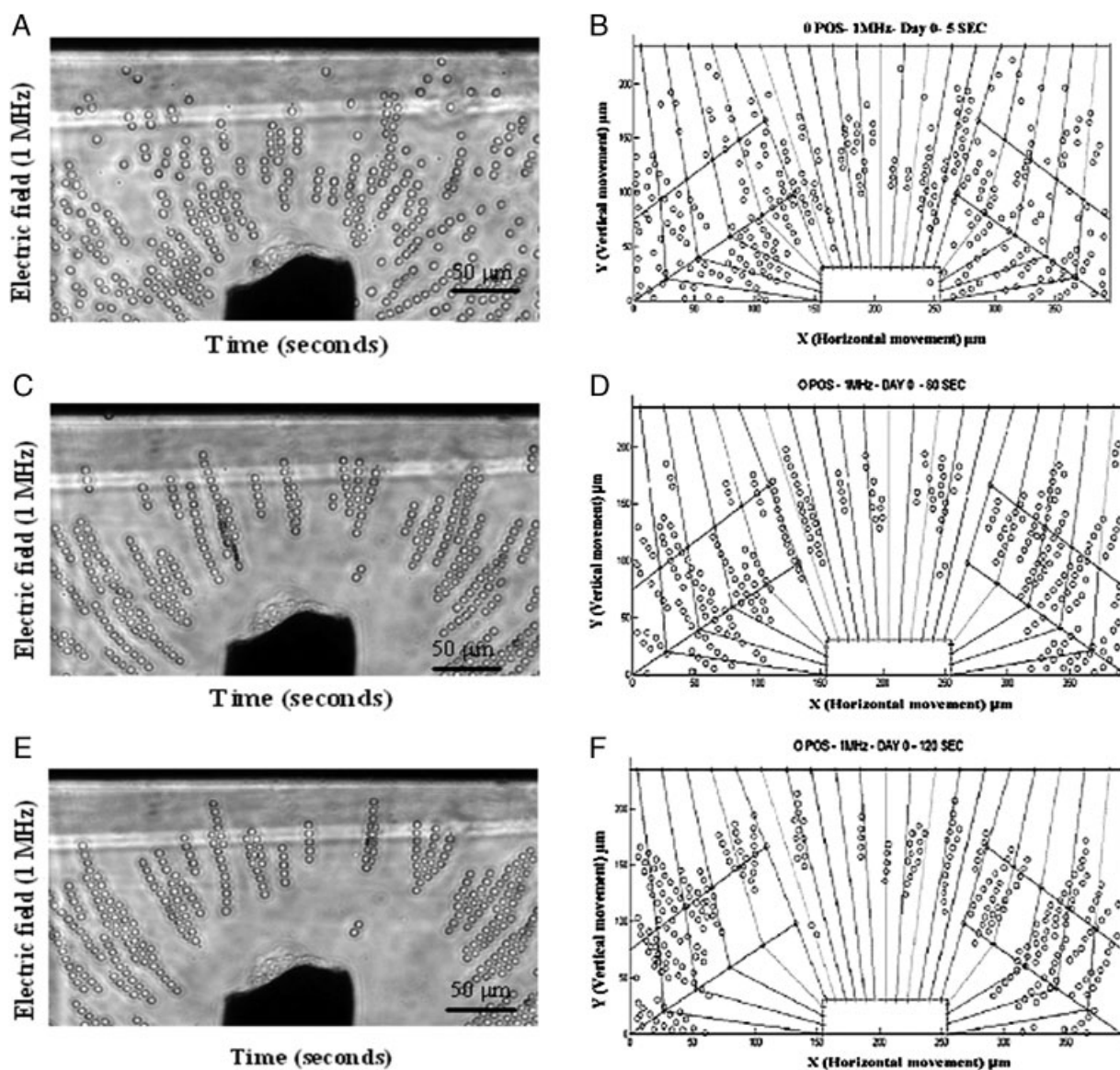


**Figure 5.** Comparison of the dielectrophoretic response of O+ blood type at times 5 s (A, B), 60 s (C, D) and 120 s (E, F) and their corresponding MATLAB representations (B, D and F) within the wedge regions, respectively. As demonstrated, the images and mapped (X, Y) cell position data from MATLAB are in good agreement.

able and robust. As demonstrated, a 1 MHz dielectrophoretic field induced a fast response (less than 2 min) of the erythrocyte suspension. In order to quantify cell movements, three specific parameters were developed: cell counts by wedge region, vertical movement and horizontal movement. These are discussed in detail in Sections 3.1 to 3.4.

### 3.1 Total cell counts by wedge region

MATLAB output for the dielectrophoretic response analysis for O+ after 120 s of field application corresponding to the MATLAB representation in Fig. 5F is shown in Figs. 6A and B. Figure 6A shows the horizontal

spacing of total number of cells in each wedge region from L to R. Significant lateral movement of cells from midfield is suggestive of negative DEP. In Fig. 6B vertical distance along the wedges was scaled from 0 to 1 with 0 located near the high field density electrode and 1 near the low field density electrode.

Total cell counts were tallied for all images analyzed (days 0, 2 and 5 and on each of those days at 0, 20, 30, 50, 60, 90 and 120 s). The percentage of cells remaining in the image field of view was averaged over two independent blood samples and compiled for all four blood types in Table 1. As shown, there was a steady decline in the total number of cells in the image field of view as the experimental runs progressed. This effect reduces the

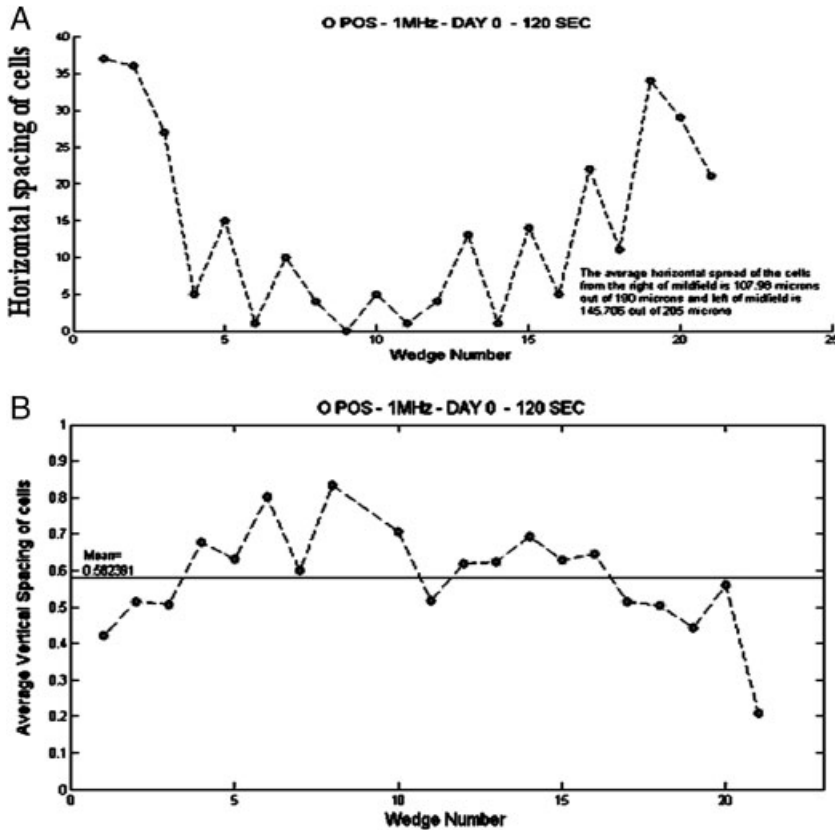


**Figure 6.** MATLAB output for the dielectrophoretic response analysis for O+ after 120 s of field application corresponding to the MATLAB representation in Fig. 5F. Figure 6A shows the horizontal spacing of total number of cells in each wedge region from L to R. Significant lateral movement of cells from midfield is suggestive of negative DEP. In Fig. 5B vertical distance along the wedges was scaled from 0 to 1 with 0 located near the high field density electrode and 1 near the low field density electrode.

**Table 1.** Percentage of cells remaining in the image field of view for all four positive blood types<sup>a)</sup>

Blood group type	Total % of cells remaining from time 0 s						
	Time (s)						
	0	20	30	50	60	90	120
A+	100	93	90	86	80	73	68
B+	100	94	90	84	80	75	69
AB+	100	94	93	88	86	83	79
O+	100	93	92	87	90	90	89

a) The percentage of cells remaining in the image field of view is compiled for all four positive blood types. There is a steady decline in the total number of cells in the field of view as the experimental run time progresses.

magnitude of the vertical and horizontal movement parameters as values computed at 90 and 120 s were based on fewer cells.

### 3.2 Vertical movement

Vertical movement captures movement of cells between the high and the low field density electrodes by tracking cell position in each wedge. It is determined by the cell's distance from the high field density electrode normalized by the total length of the wedge ( $l_j$ ). This results in a bounded

number between 0 and 1 where 0 would result when cells were clustered near the high field density region (positive DEP) while 1 reflects cells aggregating at the low field density region (negative DEP). Vertical movement,  $M_V$ , captures the movement of RBCs up or down the wedges in the dielectrophoretic field. In equation form, it is given by

$$M_V = \frac{\sum_{i=1}^W (\sum_{j=1}^n c_j / l_j) / n_i}{W} \quad (6)$$

where  $n_i$  is the total number of cells in wedge  $i$ ,  $c_j$  is the distance along the wedge path from the cell to the high field density electrode for each cell for  $j = 1$  to  $n$ ,  $l_j$  is the total length of the wedge and  $W$  is the total number of wedges. An overall vertical position was obtained by averaging positions in all the wedges. This profile is depicted in Fig. 6 where the average vertical position of the cells is shown as a function of the wedges from left to right. Wedge #11 is the middle wedge and the symmetry in the X dimension can be observed (Fig. 6b). The information was further condensed by calculating a mean across all wedges to give the average vertical movement. These data were plotted as a function of experimentation time for all blood types and are depicted in Fig. 7.

Points are shown for A+, B+, AB+ and O+ blood types and standard error is represented for each point. The standard error accounts for variability between the two independent blood samples as well as across experiment days 0, 2 and 5 since it is known that membrane fluidity of the

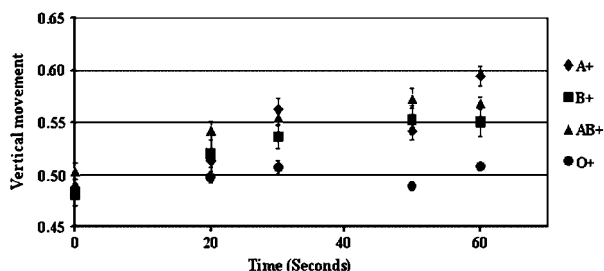


**Figure 7.** Vertical movement is calculated according to Eq. (6) and is shown as a function of experimental run time up to 60 s. Points are shown for A+, B+, AB+ and O+ blood types and standard error is represented for each point. In all cases, average cell position starts near 0.5 (halfway between electrodes). O+ hovers near 0.5 while all other blood types deviate toward the low field density electrode. The best separation achieved for all the four blood types was around 60 s. All the blood types converge back after 60 s as given in Table 1. Trend lines are not shown in the figure but are compiled in Table 2 for the experimental run time of 0–90 s.

erythrocytes does not change appreciably for the first 6 days of storage [27]. Standard errors were reasonable with values between 0.003 and 0.015 (0.6–3  $\mu\text{m}$ ) and were expected given that these were biological, micrometer scale experiments. In all cases, average cell position started near 0.5 (halfway between electrodes) corresponding to  $\sim 100 \mu\text{m}$  since a distance of 0.1 in Fig. 7 represents erythrocyte movement of about 20  $\mu\text{m}$ . O+ continued to hover near 0.5 while all other blood types deviated toward the low field density electrode region. The best separation achieved for all four blood types was at 60 s as shown in Fig. 7. All the blood types converge back to a comparable average vertical position after 60 s due to the loss of cells from the field of view. Since these numbers are artificially skewed due to the data analysis tools, only 0–60 s are analyzed further (time frame where >80% of cells exist in the field of view). The four blood types were fit to a linear trend; intercept and  $R^2$  values for each blood type are tabulated in Table 2 for experimental run time from 0 to 60 s.

Further, statistical analysis was performed as described in the data analysis section and three different tests were chosen: primary effects, interaction of primary effects and primary effects only at 60 s. First, the vertical means of primary effects, DAY, TIME and BLOOD TYPE were compared. A goodness-of-fit test was performed on the model in Eq. (4), which yielded an observed significance level ( $p$ -value) of less than 0.0001. At this  $p$ -value, a conventional threshold significance level of 0.05 was chosen to study the variance. At this corresponding confidence level of 95%, it was concluded that all or at least one of the vertical movement means were different by Fisher's least significant difference method [33]. Least significant difference is the observed difference between any pair-wise interaction effects sample means necessary to declare the corresponding population of interaction effect means different.

To know which means were different, interaction effects of (DAY\*TIME), (DAY\*BLOOD TYPE) and

**Table 2.** Linear trends of the vertical and horizontal movements for four positive blood types<sup>a)</sup>

Blood type	Slope		Intercept		$R^2$	
	Vertical	Horizontal	Vertical	Horizontal	Vertical	Horizontal
A+	0.0015	0.0012	0.49	0.54	0.78	0.91
B+	0.0011	0.0015	0.51	0.53	0.89	0.98
AB+	0.0012	0.0011	0.49	0.53	0.90	0.93
O+	0.0002	0.0008	0.49	0.53	0.28	0.95

a) The linear trends of the vertical and horizontal movements are shown for all the four positive blood types. The intercepts and slope are given along with the  $R^2$  value. These data are compiled for the experimental run time of 0–60 s for vertical movement and 0–90 s for horizontal movement as 60 and 90 s were the time where best spatial separation of all the four blood types were achieved for vertical and horizontal movements, respectively.

(TIME\*BLOOD TYPE) were compared, which is known as Multiple Comparisons carried out pair-wise [33]. Multiple comparisons of these interactions were performed using Fisher's method of least significant difference [33]. A goodness-of-fit test [33] was performed on Eq. (4), which yielded a  $p$ -value of 0.001. At this  $p$ -value, a confidence level of 95% was chosen for this interaction analysis. Significant interaction of (DAY\*BLOOD TYPE) was observed, but there was no evidence to support interactions between (TIME\*BLOOD TYPE). Multiple comparisons at an alpha of 0.05 suggested that O+ had a statistically significantly low mean vertical movement compared with the remaining blood types.

At this alpha value, there was no evidence to suggest that there was a difference between A+, B+ and AB+ blood types. In order to assess at which confidence level A+, B+ and AB+ could be discerned from each other, an iterative approach was taken. By successively decreasing the confidence level,  $\alpha$ , the confidence at which the blood types could be discerned was determined. It was found that AB+ is statistically different from B+ with a confidence of 85% and AB+ is statistically different from A+ with a confidence of 65%, which suggests that AB+ behaviors more closely mimic A+ vertical movement behavior. As given in Table 3, it was only at a confidence level of 56% that all four blood types could be reproducibly distinguished.

Practical diagnostic devices may only consider a result at one point in time. Therefore, least significant difference by multiple comparisons of primary effect, BLOOD TYPE, was also studied by examining average vertical positions at 60 s, as this was the time where best separation of all the blood types was achieved (Fig. 7). A goodness-of-fit test was again performed on Eq. (5), which yielded a  $p$ -value of 0.1172. Hence a confidence level of 85% was chosen for analysis. There was no influence of DAY on 60 s vertical movement data. At alpha of 0.15, multiple comparisons on BLOOD TYPE showed O+ to be significantly different from A+ and AB+ but not from B+. There was no evidence to suggest

**Table 3.** Least significant difference multiple comparison results for vertical movement<sup>a)</sup>

$\alpha$ -Value	Confidence level (%)	Significantly different blood types observed for vertical movement
0.05	95	O+ can be distinguished from A+, B+ and AB+
0.15	85	AB+ can be distinguished from B+
0.35	65	AB+ can be distinguished from A+
0.44	56	All four blood types can be distinguished

a) Least significant difference multiple comparison results for average vertical movement are shown. The confidence level at which the vertical movement parameter is able to distinguish blood type is tallied.

that A+, B+ and AB+ were significantly different from each other at an 85% confidence level.

Thus, the above quantitative results as well as qualitative observations suggest that vertical cell motion in a dielectrophoretic field is weakly dependent on BLOOD TYPE and that O+ dependencies are statistically significant with greater than 95% confidence, while other blood types are only significantly distinguishable at 56% confidence level.

### 3.3 Horizontal movement

The horizontal movement parameter captures the movement of erythrocytes away from the midfield toward the left or right edges of the image in the dielectrophoretic field (Fig. 4). The distance from the electrode centerline (midfield) to the image edges on either side ( $D_L$  on the left side and  $D_R$  on the right side) was measured. The horizontal distance of the cells from midfield was calculated separately for the left-hand side ( $d_L$ ) and the right-hand side ( $d_R$ ) of the image (Fig. 4). The total number of cells on either side of the centerline ( $N_L$  on the left side and  $N_R$  on the right side) were also calculated. Equation (7) shows how the position was normalized and averaged to give horizontal movement; the resulting values were plotted for each blood type as a function of time in Fig. 8. Horizontal movement,  $M_H$ , aids in assessing the movement of the RBCs either toward or away from the higher field gradient region (midfield) of the device. In equation form:

$$M_H = \frac{\sum_{i=1}^{N_L} d_L/N_L \cdot D_L + \sum_{i=1}^{N_R} d_R/N_R \cdot D_R}{2} \quad (7)$$

Data points for A+, B+, AB+ and O+ blood types are plotted with corresponding standard errors shown in Fig. 8. Standard errors were reasonable with values between 0.0025 and 0.021 (0.5–4.2  $\mu\text{m}$ ) and were expected given that these were biological, micrometer scale experiments. A distance of about 0.1 on the graph corresponded to  $\sim 20 \mu\text{m}$  on the raw images from the device. For all four blood types, initial cell position was near 0.5 (100  $\mu\text{m}$ ), which represents the distance halfway between midfield and the far left or far

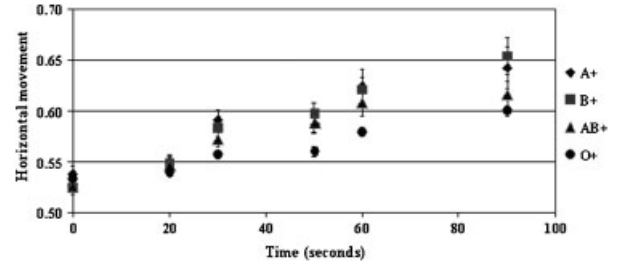


**Figure 8.** Movement in the horizontal dimension is calculated via Eq. (7). Data points for A+, B+, AB+ and O+ blood types are plotted and corresponding standard errors shown. For all four blood types, initial cell position is near 0.5, which is halfway between midfield and the far left or far right of the image. Movement with time is away from midfield in all cases. From the figure, the best separation was achieved at 90 s for all four blood types. All the blood types converge back after 90 s as given in Table 1. Trend line data are again compiled in Table 2 for the experimental run time of 0–90 s.

right of the image (Fig. 4). Movement with time was away from midfield, out of the image field of view for all four types. Type B+ cells horizontal movement was consistently greater than other blood types during the experiment from 20 to 120 s. In contrast, O+ cells demonstrated the smallest movement from midfield, which is consistent with qualitative observations (Fig. 2). From Fig. 8, the best horizontal spread achieved was at 90 s for all four blood types. As was observed with the vertical movement data, the loss of cells from the field of view artificially skewed the quantified position values, so only 0–90 s data were analyzed further. The four blood types converge back after 90 s and all blood types followed a linear trend; intercept and  $R^2$  values for each blood type are tabulated in Table 2 for experimental run time from 0 to 90 s.

Further, statistical analysis was performed as previously described. First, the horizontal means of primary effects, DAY, TIME and BLOOD TYPE were compared. A goodness-of-fit test was performed on the model in Eq. (4), which yielded an observed significance level ( $p$ -value) of less than 0.0001. As before, a threshold significance level of 0.05 was chosen to study the variance. At this 95% confidence level, it was concluded that all or at least one of the horizontal movement means were different by Fisher's least significant difference method [33]. To know which means were different on the primary effects, interaction effects of (DAY\*TIME), (DAY\*BLOOD TYPE) and (TIME\*BLOOD TYPE) were compared and significant interactions were observed for all the three interactions. By this method, DAY 0 was significantly different from 2 and 5. TIME periods 0, 90 and 120 were significantly different from the other periods. This means that dielectrophoretic response is measurable at 0 and 90 s, and at 120 s, the total number of cells in the field of view are significantly impacting the profile of horizontal movement (see Table 1). The horizontal movement at other times of 20 and 60 s showed indistinguishable behaviors. It also showed that BLOOD TYPE O+ was significantly different from A+ and B+ but not from

**Table 4.** Least significant difference multiple comparison results for horizontal movement<sup>a)</sup>

$\alpha$ -Value	Confidence level (%)	Significantly different blood types observed for horizontal movement
0.05	95	O+ can be distinguished from A+ and B+
0.15	85	O+ can be distinguished from AB+
0.25	75	AB+ can be distinguished from A+ and B+
0.92	8	All four blood types can be distinguished

a) Least significant difference multiple comparison results for horizontal movement are shown. The confidence level at which the horizontal movement parameter is able to distinguish blood type is tallied.

AB+ at a 95% confidence level. The confidence level,  $\alpha$ , was successively decreased until a level was reached where the blood types could be discerned. With 85% confidence, O+ could be discerned from AB+ by examining horizontal movement. At 75% confidence, AB+ could be distinguished from A+ and B+, but it was only with 8% confidence that all four positive blood types could be distinguished by examining horizontal movement alone. These data are given in Table 4.

Again, to assess robustness if only one data point was used in a diagnostic device, the primary effect (BLOOD TYPE) was studied at 90 s, as this was the time where best spatial separation of all the blood types was achieved (Fig. 8). A goodness-of-fit test [33] was performed on the model in Eq. (5), which yielded a  $p$ -value of 0.2718 so  $\alpha$  of 0.3 was chosen for further analysis. At this 70% confidence level, all blood types were the same with the multiple comparison tests and there was no evidence to suggest that day or blood type were significantly influencing the horizontal movement values.

The statistical analysis conducted neglects the influence of the substantial number of cells that are lost from the analysis field of view. The impact of this is primarily on the horizontal movement because as the cells approach the edge of the field of view, their position drives the average up, but as they move out of the field of view, the average drops. This is likely the reason that blood type is discernable with horizontal movement at lower confidence levels than with the vertical movement tracking alone. Analyzing a large image space would likely help in addressing this issue. Thus, we can conclude that horizontal movement is not substantial enough to distinguish blood types, but that tracking of vertical movement is far more reliable.

### 3.4 Composite distance

The distance parameter captures the composite movement of erythrocytes in both the horizontal and vertical directions. This parameter is calculated using the distance formula with the vertical positions,  $M_V$ , and horizontal positions,  $M_H$ ,

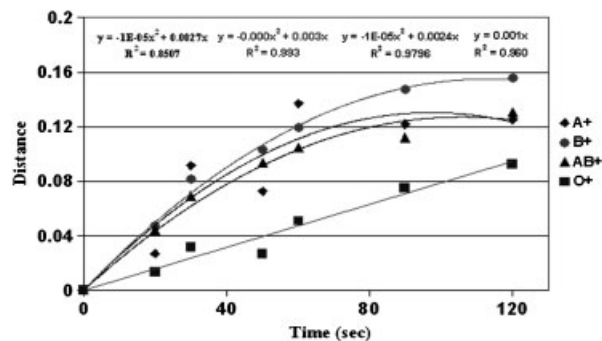


**Figure 9.** Composite distance combining horizontal and vertical movement figures *via* the distance formula in Eq. (8). Distance increases with time away from image center for A+, B+, AB+ and O+ blood types. From the figure, A+, B+ and AB+ movements cease to appreciably change after approximately 90 s due to the loss of cells from the analysis area as given in Table 1.

always calculated as relative to the initial average position at time 0 as follows:

$$D_{xy} = \sqrt{(M_V^{\text{time}0} - M_V)^2 + (M_H^{\text{time}0} - M_H)^2} \quad (8)$$

This parameter allows to represent total movement in one number as a function of time. The resulting distances traveled are given in Fig. 9 along with fitted trend lines. Distance increases with time away from image center for all blood types. O+ cell distances followed a nice linear trend with an  $R^2$  of 0.96, while A+, B+ and AB+ cell types all required second-order polynomial fits to attain acceptable  $R^2$  values. B+ and AB+ erythrocytes polynomial fits are 0.99 and 0.98, respectively. However, A+ blood type result varies and the fit is only good to an  $R^2$  value of 0.85. The need for a second-order polynomial to estimate the trend of the data is necessary due to the loss of cells from the image field of view and thus the analysis area. From Fig. 9, A+, B+ and AB+ erythrocyte movements cease to appreciably change after approximately 90 s due to the loss of cells from the analysis area as given in Table 1. This causes a tapering off of the measured movement from the highest field density regions. This movement differs from that predicted by traditional dielectrophoretic theory (Eqs. 1 and 2) suggesting that the polysaccharide antigens on the red blood surface impact the dielectrophoretic response. The single distance parameter demonstrates the same movement patterns noted in the individual vertical and horizontal movement data and is a good tool for tracking blood cell motion in dielectrophoretic fields.

As demonstrated in Fig. 2 and verified in analysis (Figs. 7–9), the dielectrophoretic responses of A+, B+ and AB+ blood types were similar to each other but differentiable from O+ blood type. The O+ blood type lacks both the antigens A and B and this may be the reason for the attenuated dielectrophoretic response to the applied field. The A and B antigens have a similar structure in terms of their modification of the H glycoconjugate [27, 28],

*N*-acetyl-galactosamine and *N*-acetyl-glucosamine, respectively. The horizontal and vertical movement tracking showed different trends in the dielectrophoretic movement of erythrocytes for A+, B+, AB+ and O+ blood types with time. Also, dielectrophoretic response of the O+ and AB+ blood types can be differentiated easily with greater than 95% confidence from vertical movement alone. This is of particular significance since O+ blood type, a universal donor (can be transfused to a person of any blood type) and AB+, a universal acceptor (can take any blood type *via* transfusion). Cells of O+ blood type were the least responsive to the dielectrophoretic field, while cells of the A+ blood type showed greatest response with time. This work, once improved upon, is significant for emergency blood transfusion applications and also in portable blood typing device for easy and rapid blood diagnostics.

#### 4 Concluding remarks

Collectively, dielectrophoretic movement of erythrocytes in the vertical and horizontal directions depends significantly on blood type. The dielectrophoretic movement of each positive blood type was seen to follow distinct trends with time. The parameters, total cell count, vertical movement, horizontal movement and distance were used to capture the total cells, and movements of the erythrocytes in each wedge in the dielectrophoretic field. From Table 1, for O+ blood type the total cells remaining in the field of view was about 90% without much change throughout the experimental run time, but drastic decreases in the total cells within the analysis window was observed for both A+ and B+ blood types. In case of AB+ blood type, the total cells remaining were in-between O+ and A+, B+ blood types. Vertical and horizontal movements indicated the best separation times to be 60 and 90 s, respectively, for all the blood types. The combined distance parameter illustrated this trend as was expected with the data following a linear trend away from dielectrophoretic field center before stabilizing off due to cell loss.

All parameters showed that O+ had an attenuated response compared with all other blood types. This was also verified from the statistical analysis on vertical and horizontal movements by Fisher's least significance difference method. At 95% confidence level, vertical movement showed O+ to be different from the other three types. O+ erythrocytes also showed relatively attenuated responses likely due to the absence of two antigens and this has large implications as type O blood is a universal donor. Also, A+ and B+ have very similar responses in the dielectrophoretic field with AB+ demonstrating similar spatial distributions. With both vertical and horizontal movement parameters and subsequently combined distance, AB+ demonstrated values between those shown by A+, B+ and O+. This is due to the fact that A+, B+ and AB+ all are having antigens that are structurally similar [29] differing only by their side chains,

on the polysaccharide backbone. AB+ responses differed from A+ and B+ likely because AB+ erythrocytes express both A and B glycoforms on their membrane. Wedge binning approach *via* MATLAB and statistical analysis *via* SAS were able to capture the difference in the dielectrophoretic response of the RBCs of different positive blood types.

The use of microdevices for blood typing can help increase the speed and efficiency of emergency medical diagnosis. Current blood typing technologies require time, a clinical environment, and antibody assays for each blood type; such medical technological methodologies require skilled medical technicians and are not readily portable to emergency sites, which make the whole testing method more expensive and prone to false positives and negatives. DEP shows excellent potential for this purpose as it has many advantages over conventional blood typing techniques, spectroscopy and magnetophoresis. We have demonstrated the capacity of DEP as an analytical tool to differentiate positive blood types without any pretreatment or cell modification beyond simple dilution. Four parameters were used to capture the differences in the dielectrophoretic movement of the erythrocytes based on their blood types: total cell count, vertical movement, horizontal movement and combined distance. All parameters showed that O+ had an attenuated response compared with all other blood types. At 95% confidence level, vertical movement showed O+ to be different from the other three types with A+ and B+ having similar responses in the dielectrophoretic field with AB+ tracking close by. This work provides preliminary evidence that dielectrophoretic responses are influenced by the expression of polysaccharide molecules on the surface of cells, which has ramifications for future studies of the dielectrophoretic behavior of other biological cells. The current work is limited because it does not account for all the antigens on the blood cell surface, only ABO antigens. The results are accurate with acceptable standard errors, which is especially gratifying given that custom-made microdevices with electrode variability were utilized. Further work must be done to study the dielectrophoretic response of negative blood types as well as field dependency and frequency dependency of the dielectrophoretic movement of all blood types. A pragmatic method for using this information for a commercial microdevice is also to be studied where analysis is performed using analytical equipment.

*The authors gratefully acknowledge Longest Student Health Center, Mississippi State University for obtaining blood samples from donors whenever required and also various volunteers, whose names have been kept anonymous due to regulations, for donating their blood. The authors would also like to thank Dr. Mark Bricka for his advice and support on Statistical Analysis Software (SAS). This research was supported by NSF CAREER 0644538.*

*The authors have declared no conflict of interest.*

## 5 References

- [1] Nishi, K., Rand, S., Nakagawa, T., Yamamoto, A. *et al.*, *Anil Aggrawal's Internet J. Forensic Med. Toxicol.* 2005, 6.
- [2] Narayanan, S., Galloway, L., Nanoyama, A., Leparo, G. F. *et al.*, *Transfusion* 2002, 42, 619–626.
- [3] Soper, S. A., Hashimoto, M., Situma, C., Murphy, M. C. *et al.*, *Methods* 2005, 37, 103–113.
- [4] Zborowski, M., Ostera, G. R., Moore, L. M., Milliron, S. *et al.*, *Biophys. J.* 2003, 84, 2638–2645.
- [5] Minerick, A. R., Zhou, R., Takshistov, P., Chang, H. C., *Electrophoresis* 2003, 24, 3703–3717.
- [6] Gascoyne, P., Mahidol, C., Ruchirawat, M., Satayavivad, J. *et al.*, *Lab Chip* 2002, 2, 70–75.
- [7] Pethig, R., Huang, Y., Wang, X., Burt, J. P. H., *J. Phys. D. Appl. Phys.* 1992, 24, 881–888.
- [8] Cheng, J., Sheldon, E. L., Wu, L., Uribe, A. *et al.*, *Nat. Biotechnol.* 1998, 16, 541–546.
- [9] Helmke, B. P., Minerick, A. R., *Proc. Natl. Acad. Sci. USA* 2006, 103, 6419–6424.
- [10] Ugaz, V. M., Brahmasandra, S. N., Burke, D. T., Burns, M. A., *Electrophoresis* 2002, 23, 1450–1459.
- [11] Biomedical-Lab Equipment, Hematology, <http://websites.labx.com/rankin/listings.cfm?show=1&catid=1282> (accessed in February 2008).
- [12] Cohen, J., Monitoring treatment: at what cost?, *Science* 2004, 304, 1936.
- [13] American Sickle Cell Anemia Association (ASCAA), *How common is sickle cell anemia*, [http://www.ascaa.org/How\\_Common\\_Is\\_Sickle\\_Cell\\_Anemia.asp](http://www.ascaa.org/How_Common_Is_Sickle_Cell_Anemia.asp) (accessed in February 2008).
- [14] Edvotek, *The biotechnology education company, "Genetically inherited disease detection kit"*, <http://www.edvotek.com/116.html> (accessed in February 2008).
- [15] Pohl, H., *Dielectrophoresis: The Behavior of Neutral Matter in Nonuniform Electric Fields*, Cambridge University Press, New York, NY 1978.
- [16] Pethig, R., *Crit. Rev. Biotechnol.* 1996, 16, 331–348.
- [17] Gheorghiu, E., *Ann. NY Acad. Sci.* 1999, 873, 262–268.
- [18] Vrinceanu, D., Gheorghiu, E., *Bioelectrochem. Bioenerg.* 1996, 40, 167–170.
- [19] Gheorghiu, E., Asami, K., *Bioelectrochem. Bioenerg.* 1998, 45, 139–143.
- [20] Becker, F. F., Wang, X. B., Pethig, R., Gascoyne, P. R. C. *et al.*, *J. Phys. D Appl. Phys.* 1994, 27, 2659–2662.
- [21] Sancho, M., Martinez, G., Martin, C., *J. Electrostatics* 2003, 57, 143–156.
- [22] Becker, F. F., Wang, X. B., Pethig, R., Gascoyne, P. R. C. *et al.*, *Proc. Natl. Acad. Sci. USA* 1995, 92, 860–864.
- [23] Gascoyne, P., Pethig, R., Satayavivad, J., Becker, F. F. *et al.*, *Biochem. Biophys. Acta* 1997, 1323, 240–252.
- [24] Borgatti, M., Altomare, L., Baruffa, M., Fabbri, E. *et al.*, *Int. J. Mol. Med.* 2005, 15, 913–920.
- [25] Yuang, J., Wang, X., Becker, F. F., Gascoyne, P. R. C., *Biophys. J.* 2000, 78, 2680–2689.
- [26] Daniels, G., Bromilow, I., *Essentials Guide to Blood Groups*, Blackwell Publishing, Oxford 2007.
- [27] Patenaude, S. I., Sato, N. O. L., Borisova, S. N., Szpacenko, A., *Nat. Struct. Biol.* 2002, 9, 685–690.
- [28] Goldin, C., Caprani, A., *Eur. Biophys. J.* 1997, 26, 175–182.
- [29] Sheffield, P. W., Tinmouth, A., Branch, D. R., *Transfus. Med. Rev.* 2005, 19, 295–307.
- [30] Draper, C. J., Greenwalt, T. J., Dumaswala, U. J., *Transfusion* 2002, 42, 830–835.
- [31] COMSOL-Multiphysics Modeling, version 3.3, <http://www.comsol.com/> (accessed in June 2008).
- [32] SAS – Statistical Analysis Software, version 9.1, <http://www.sas.com/> (accessed in February 2008).
- [33] Ott, L. R., Longnecker, M., *An Introduction to Statistical Methods and Data Analysis*, Thompson Learning, Inc., 5th Edn., 2001.